The first structure of pectate lyase belonging to polysaccharide lyase family 3

Masatake Akita,[a]***** **Atsuo Suzuki,**[a] **Tohru Kobayashi,**[b] **Susumu Ito**[b] **and Takashi Yamane**[a]

[a]Department of Biotechnology and Biomaterial Chemistry, Graduate School of Engineering, Nagoya University, Chikusa-ku, Nagoya 464-8603, Japan, and [b]Tochigi Research Laboratories of Kao Corporation, 2606 Akabane, Ichikai, Haga, Tochigi 321-3497, Japan

Correspondence e-mail:
h991401d@mbox.media.nagoya-u.ac.jp

The crystal structure of a highly alkaline low molecular weight pectate lyase (Pel-15) was determined at 1.5 Å resolution by the multiple isomorphous replacement (MIR) method. This is the first pectate lyase structure from polysaccharide lyase family 3. The overall structure is a simple eight-turn right-handed parallel β-helix domain with one long loop protruding from one side of the β-helix. The low molecular weight of Pel-15 derives from the lack of N- and C-terminal extensions that are found in many β-helix proteins. Although the structure has one calcium ion at pH 6.7, raising the pH to 9.5 results in the binding of an additional calcium ion. The common calcium ion found in both the pH 6.5 and 9.5 structures seems to stabilize both the β-helix structure and the long protruding loop. The additional calcium ion found in the pH 9.5 structure alone may neutralize the acidic substrate. The region around the additional calcium ion is thought to bind to the substrate, as this region is rich in charged amino-acid residues which are required in catalysis.

1. Introduction

Pectate lyases (Pel; E.C. 4.2.2.2) catalyze the degradation of the pectate component of the middle lamellae and cell walls of higher plants. The enzymes are secreted by bacteria and fungal pathogens and cause soft-rot diseases in higher plant cells. Generally, Pels degrade polygalacturonic acid (PGA) through a β-elimination mechanism with the assistance of Ca^{2+} ions at pHs between 8 and 10.

Bacillus sp. strain KSM-P15 produces a low molecular-weight highly alkaline Pel (Pel-15) in an alkaline culture. The molecular weight of Pel-15 is 20 924 Da with 197 amino-acid residues (Kobayashi *et al.*, 1999) and the enzyme was classified into polysaccharide lyase family 3 (Coutinho & Henrissat, 2000). Pel-15 has the highest optimal pH (10.5) of the Pels that have been reported thus far. In the enzymes belonging to polysaccharide lyase family 3, a highly conserved region exists in the region between residues 36 and 132 in Pel-15 nomenclature (Hatada *et al.*, 2000). The sequence identity of the conserved region of Pel-15 is in the range 40.5–79.4% when compared with those of PelA, PelB, PelC and PelD from *Fusarium solani* f. sp. *pisi* (González-Candelas & Kolattukudy, 1992; Guo *et al.*, 1995a,b, 1996), PelB from *Erwinia carotovora* ssp. *carotovora* (Heikinheimo *et al.*, 1995), PelI from *E. chrysanthemi* (Shevchik *et al.*, 1997) and PelA from *Bacillus* strain BP-23 (Soliano *et al.*, 2000). In contrast, when Pel-15 is compared with structurally known Pels from polysaccharide lyase family 1 (Coutinho & Henrissat, 2000; Henrissat *et al.*, 1995), such as *E. chrysanthemi* pectate lyase C (Ech-PelC; Yoder, Keen *et al.*, 1993; Yoder, Lietzke *et al.*, 1993),

E. chrysanthemi pectate lyase E (Ech-PelE; Yoder, Lietzke *et al.*, 1993; Lietzke *et al.*, 1996) and *Bacillus subtilis* pectate lyase (BsPel; Pickersgill *et al.*, 1994), the sequence identity is 20.4% at most.

One of the major goals of the structural study of Pel-15 is to discover whether there is structural homology between the enzymes in polysaccharide lyase families 1 and 3. The crystal structures of several Pels in polysaccharide lyase family 1 have been reported thus far. They have a unique structural domain, designated a β-helix (Yoder, Keen *et al.*, 1993). The β-helix structure is found not only in pectate lyases but also in other polysaccharide-binding enzymes/proteins such as *Salmonella typhymurium* phage P22 tailspike protein (Steinbacher *et al.*, 1994), *E. carotovora* sp. *carotovora* polygalacturonase (Pickersgill *et al.*, 1998), *Aspergillus niger* endopolygalacturonase II (Santen *et al.*, 1999), *A. aculeatus* rhamnogalacturonase A (Peterson *et al.*, 1997), *Flavobacterium heparium* chondroitinase B (Huang *et al.*, 1999) and *Bordetella pertussis* pertactin (Emsley *et al.*, 1996). Differences in the β-helix structures arise from the lengths of the long loops that connect the β-sheets composing the β-helix structure. These L- or V-shaped right-handed β-helix proteins have characteristically large molecular weights (over 350 residues). Therefore, it is interesting to find that the Pel-15 molecule, with fewer than 200 residues, has a folded β-helix structure.

This paper is primarily concerned with the crystal structure of Pel-15, which belongs to a new class of polysaccharide lyases, family 3. The derived structure is compared with another structurally known Pel, Ech-PelC, with respect to the role of calcium ions and the geometry of the catalytic residues. Moreover, the overall structure of Pel-15 is compared with those of other structurally known β-helix enzymes/proteins.

2. Materials and methods

2.1. Determination of pH 6.5 crystal structures

2.1.1. Isolation, purification and crystallization. The isolation and purification of Pel-15 was performed as described previously (Kobayashi *et al.*, 1999). Crystallization conditions and preliminary crystallographic studies of Pel-15 have been published previously (Akita *et al.*, 2000). Pel-15 has two crystal forms, form I and form II, although they are crystallized under the same conditions: 28%(w/v) polyethylene glycol 8000 in MES buffer pH 6.7. Both of them belong to the orthorhombic space group $P2_12_12_1$. The unit-cell parameters of form I are $a = 43.2$ (2), $b = 60.2$ (2), $c = 82.2$ (2) Å; those of form II are $a = 42.9$ (1), $b = 43.4$ (1), $c = 105.9$ (3) Å.

2.1.2. Data collection and processing. The form I crystal was used to determine the crystal structure by the MIR method. Heavy-atom derivatives were prepared by soaking the crystals in 1.5 mM K$_3$IrCl$_6$ and 10.0 mM K$_2$PtCl$_4$ for 25 and 5 h, respectively. X-ray data were collected from the native and derivatives of form I crystals at 100 K using a Rigaku R-AXIS IV detector system on a Rigaku RU-300 rotating-anode generator with double focusing-mirror monochromated Cu $K\alpha$ radiation. Data to 1.5 Å resolution were collected using synchrotron radiation at beamline BL-6A in the Photon Factory. X-ray diffraction data from form II crystals were also collected at 100 K. All of the collected data sets were processed using *DENZO* and *SCALEPACK* (Otwinowski, 1993). Data-collection statistics are given in Table 1.

2.1.3. Structure determination and refinement. The structure of the Pel-15 form I crystal was determined by the following method. The data sets of two derivatives were each scaled against the native data set and the sites of heavy atoms were determined with *RSPS* (Knight, 2000). The phases of the protein were refined using *MLPHARE* (Otwinowski, 1991). The calculated 3.4 Å map was improved with *DM* (Cowtan, 1994). A model was built of about half of the structure and molecular-dynamics refinement using *X-PLOR* (Brünger, 1992) was performed. The model was then rebuilt using a phase-combined map calculated with *SIGMAA* (Read, 1990). After several cycles of model refinement and rebuilding, water molecules were added to the model. The crystal structure of form II was determined by the molecular-replacement method with *AMoRe* (Navaza, 1994), using form I coordinates without water molecules. The model was refined with *X-PLOR* and water molecules were added to the model by the same procedures as those for form I. These two crystal forms had

Table 1
Data-collection and refinement statistics.

Data set	Native 1	K$_3$IrCl$_6$	K$_2$PtCl$_4$	Native 2	pH 9.5
Space group	$P2_12_12_1$	$P2_12_12_1$	$P2_12_12_1$	$P2_12_12_1$	$P2_12_12_1$
Unit-cell parameters (Å)					
a	43.2	43.0	43.4	42.9	43.3
b	60.2	60.5	59.9	43.4	43.6
c	82.2	82.6	81.0	105.9	106.9
Resolution range (Å)	20.0–2.3	20.0–3.0	20.0–3.5	20.0–1.5	20.0–2.5
Unique reflections	10063	4505	2871	30234	7049
Completeness (%)	99.3	94.7	98.2	91.2	93.8
R_{merge}†	0.069	0.094	0.127	0.034	0.047
Phasing power‡ (centric/acentric)		2.42/2.92	1.22/1.43		
FOM§		0.59 for 3001 reflections (15–3.4 Å)			
R factor¶ (R_{free})	0.186 (0.234)			0.167 (0.196)	0.193 (0.275)
R.m.s. deviation from ideal					
Bond length (Å)	0.014			0.008	0.004
Bond angles (°)	2.7			1.4	1.3
Average B factors (Å^2)					
Main chain	6.5			7.0	18.3
Side chain	7.2			8.3	18.8
Solvent oxygen	21.1			20.6	25.0
Ca^{2+} ion (near Asp80)	18.5			12.7	18.9
Ca^{2+} ion (near Glu83)					20.3

† $R_{merge} = \sum_{hkl} \sum_i |I_i(hkl) - \langle I_i(hkl)\rangle| / \sum_{hkl} \sum_i I_i(hkl)$. ‡ Phasing power = $F_H / [k(|F_{PH}|_{obs}) - (|F_{PH}|_{calc})]$. § Figure of merit, FOM = $|F(hkl)_{best}| / |F(hkl)|$, where $F(hkl)_{best} = \sum_\alpha P(\alpha) F_{hkl}(\alpha) / \sum_\alpha P(\alpha)$. ¶ R factor = $\sum_{hkl} ||F_{obs}| - k|F_{calc}|| / \sum_{hkl} |F_{obs}|$.

different molecular packings from each other and hence the amino-acid side chains, whose orientations are ambiguous because of poor electron densities, differed between the crystal forms. The undetermined side-chain orientations for the form I crystal structure were Glu7, Lys20, Asn39 and Lys185 and those for the form II crystal structure were Arg10, Lys20, Glu38, Asn39, Lys41 and Lys185. Moreover, the N-terminal residue (Ala1) of the form II model was missing. Each structure had a strong peak in the $2F_o - F_c$ electron-density map near Asp80. The distances between the peak and liganded O atoms were in the range 2.45–2.65 Å, which was close to that found in α-amylase from *B. subtilis* (Fujimoto *et al.*, 1998). Therefore, this peak was attributed to a calcium ion. Refinement statistics for both models are given in Table 1. A Ramachandran analysis using *PROCHECK* (Laskowski *et al.*, 1993) showed that 86.9% of the residues are in the most favoured regions, 11.9% are in the additionally allowed regions, 0.6% are in the generously allowed regions and 0.6% are in the disallowed regions for form I. For form II, 88.1% of the residues are in the most favoured regions, 10.7% are in the additionally allowed regions, 1.2% are in the generously allowed regions and none are in the disallowed regions. The majority of the discussions in this paper are in reference to the high-resolution structure of the form II crystal.

2.2. Preparation, data collection and structure determination of pH 9.5 crystal

The Pel-15 crystal at pH 9.5 was prepared by the following method. Form II crystals grown in the pH 6.5 crystallization solution were soaked in Tris buffer pH 8.0 with 28%(w/v) polyethylene glycol 8000 and 10 m*M* CaCl$_2$ for 1 h. The crystals were then transferred to the final solution [glycine buffer pH 9.5 with 28%(w/v) polyethylene glycol 8000 and 10 m*M* CaCl$_2$]. After the crystals had been soaked for 1 h, they were frozen using liquid nitrogen. X-ray data collection from the pH 9.5 crystal was performed at 100 K using a Rigaku R-AXIS IV detector system on a Rigaku RU-300 rotating-anode generator. The data sets to 2.5 Å resolution were processed using *DENZO* and *SCALEPACK* (Otwinowski, 1993). The crystal structure was determined by the molecular-replacement method with *AMoRe* (Navaza, 1994), using 1.5 Å resolution form II coordinates without water molecules. The pH 9.5 structure had two strong peaks in the $2F_o - F_c$ electron-density map. One peak was located at the same position as found in the pH 6.5 structure, but the other was located at a different position. This peak was attributed to the second calcium ion for the following reasons. The peak was located near the acidic residue cluster formed by Asp63,
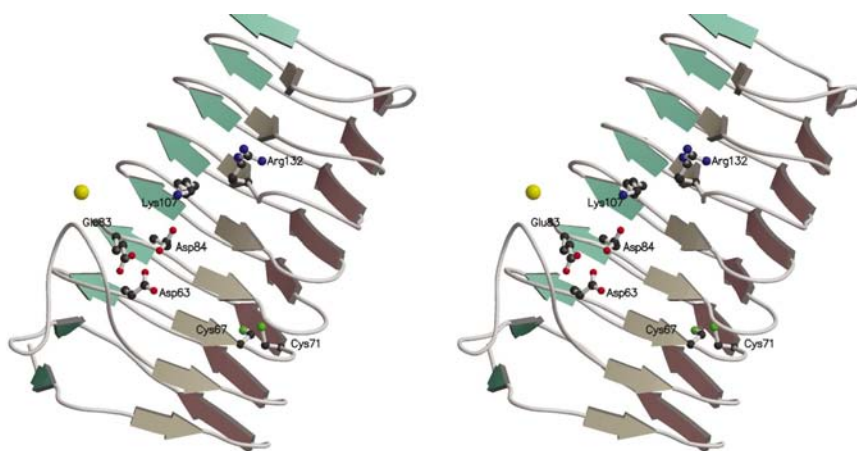

Figure 1
Stereo schematic diagram of the overall structure of Pel-15. Arrows represent β-strands. Parallel β-sheet 1 (PB1) is grey, PB2 is brownish purple and PB3 is aqua. The large yellow sphere represents the calcium ion unique to Pel-15. Amino-acid side chains are represented by ball-and-stick models. This figure and Figs. 3, 4 and 5 were prepared with *MOLSCRIPT* (Kraulis, 1991) and *Raster3D* (Merritt & Bacon, 1997).

Figure 2
Sequence alignment of Pel-15. Boxed residues are parts of β-sheets. Underlined residues are highlighted in the text.

Glu83 and Glu84. The soaking solution contained calcium ion. The *B* factor of the calcium ion was close to those of the atoms around the calcium ion. Model refinement was performed as described in §2.1.3. In the refined state, it is found that the carboxyl group of the side chain of Glu83, which was one of the ligands of the second calcium ion, was largely displaced from its position in the pH 6.5 structure. The refinement statistics are given in Table 1 ('pH 9.5'). A Ramachandran analysis in *PROCHECK* (Laskowski *et al.*, 1993) showed that 83.3% of the residues are in the most favoured regions, 15.5% are in the additionally allowed regions, 1.2% are in the generously allowed regions and none are in the disallowed regions.

3. Results and discussion

3.1. Overall structure

The overall structure of the Pel-15 molecule is a simple eight-turn parallel β-helix with no α-helix (Fig. 1). Fig. 2 shows the amino-acid sequence of Pel-15 divided into helical turns. The turn numbers in the following description refer to the nomenclature of Fig. 2. Each turn of the β-helix contains three β-strands, designated PB1, PB2 and PB3. The numbers of

residues in PB1, PB2 and PB3 are 2–3, 2–5 and 2–3, respectively. These three β-strands are connected by three turn regions: T1, T2 and T3. Consequently, one helical turn consists of a PB1-T1-PB2-T2-PB3-T3 motif. The single helical turn
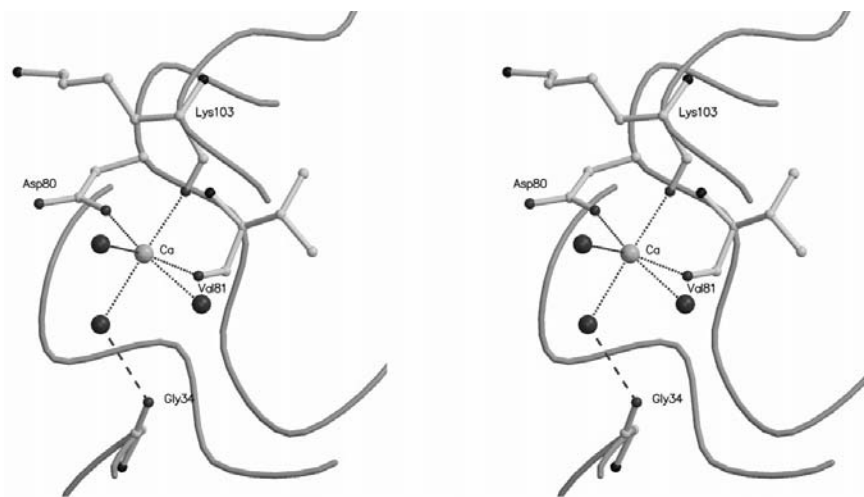

Figure 3
Stereoview of the Pel-15 unique calcium-binding site formed by Asp80, Val81, Lys103 and three water molecules. One calcium-bound water molecule is bound to the O atom of Gly34 on the first T3. The location of this region is shown in Fig. 1.
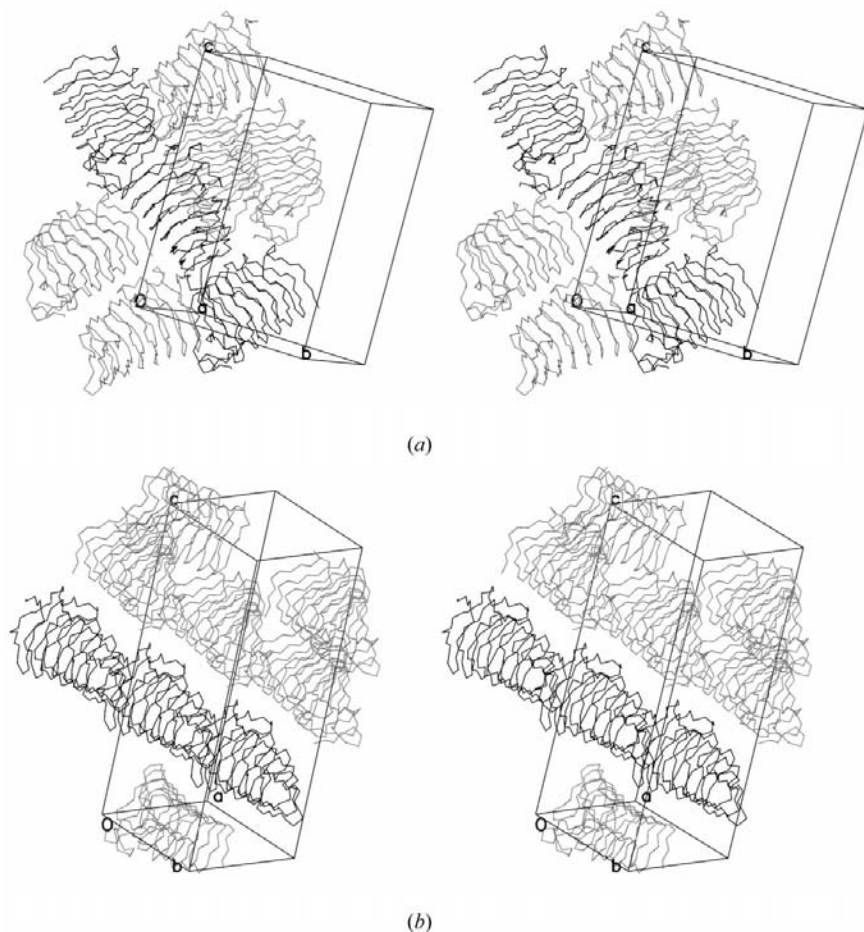

Figure 4
Stereoviews of crystal packing of (a) form I and (b) form II.

forms an L-shape; therefore, a groove is formed between T3 and PB1 (T3-PB1 groove). The T2 turns of the first and eighth helical turns consist of four residues, whereas the other T2 turns consist of two residues. The first residue of T2 has an α_L conformation, but this is not so for T2 in the fourth helical turn consisting of Gly98 and Gly99. In contrast to the regularity of T2, the lengths of T1 and T3 are variable. The number of residues in T1 is in the range 3–9 and that in T3 is in the range 4–18 (except for the last T3). T3 in the first helical turn is the longest loop region, consisting of 18 amino-acid residues with one calcium ion octahedrally liganded by six O atoms. The ligands of this calcium ion are Asp80 O^{δ} on T3 in the third helical turn, two carbonyl O atoms in the main chain (Val81 O on T3 in the third helical turn and Lys103 O on T3 in the fourth helical turn) and three water molecules (Fig. 3).

Inside the β-helix of Pel-15, a disulfide bond is found between Cys67 on PB1 and Cys71 on PB2 in the third helical turn. The disulfide bond is located inside the β-helix structure and connects the adjacent β-strands face to face (Fig. 1).

3.2. Crystal packing

The crystal structure of the form I and the form II crystals are shown in Fig. 4. The molecular structures in the two crystal forms are almost identical. In the form I crystal, the β-helix axis of one molecule is vertical or parallel to that of a symmetry-related molecule. In the form II crystal, however, the β-helix axis of one molecule is parallel to that of another molecule. Moreover, the β-helix axis of each molecule in the form II crystal is also parallel to the *a* axis of the unit cell. The adjacent molecules, which are shown in thick lines in Fig. 4, have interactions between the N-terminal helical coil of one molecule and the C-terminal helical coil of another molecule. The N- and C-terminal helical coils of the Pel-15 molecule are hydrophobic because these termini are not covered by any extension loops. Therefore, the hydrophobic interaction is most important in the growth of the form II crystals.

Adding $CaCl_2$ or EDTA to the crystallization solution enabled further investigation of these crystal forms. Crystals grown with 5 mM $CaCl_2$ grew in form I. On
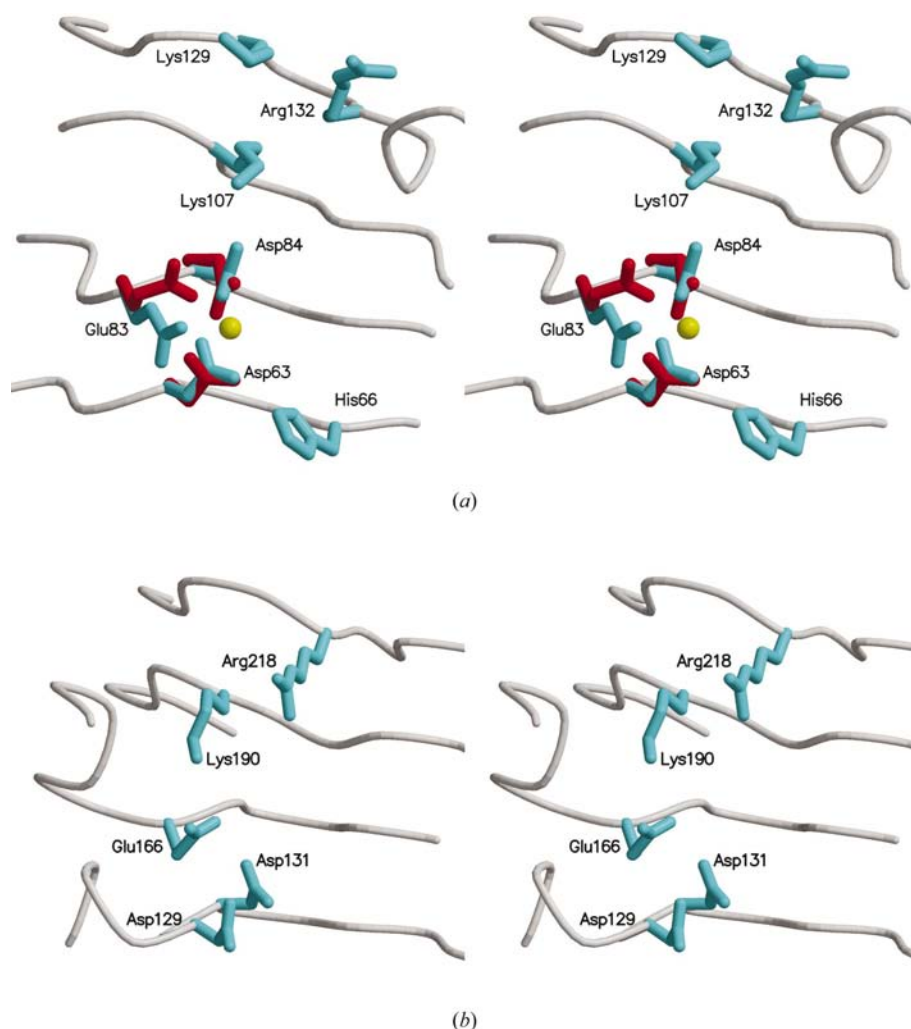
Figure 5
Stereoviews of the T3-PB1 groove regions of (a) Pel-15 and (b) Ech-PelC (PDB entry 1air). The location of this region is shown in Fig. 1. Amino-acid side chains are represented by stick models. The calcium ion and amino-acid side chains in the pH 9.5 structure are represented by a yellow sphere and red sticks, respectively. The conformations of those amino-acid side chains are changed by attachment of the calcium ion.

has two disulfide bonds, they are not located in the β-helix domain.

Another feature is the absence of characteristic amino-acid side-chain stacks found in Ech-PelC, such as the asparagine stack (designated an asparagine ladder; Yoder, Keen et al., 1993), the serine stack and the ringed-residue stack. The lack of the asparagine ladder is an especially important characteristic of the Pel-15 β-helix. In Ech-PelC, the asparagine residue of T2 tends to be present in the second position of T2 (Heffron et al., 1998). These asparagine residues are oriented inside the β-helix, resulting in the characteristic asparagine ladder. However, in Pel-15 the asparagine residue of T2 tends to be present in the first position of T2 (Fig. 2). The side chains of these asparagine residues in Pel-15 are oriented outside the β-helix.

3.3.2. Calcium binding. It is thought that a calcium ion is essential for the catalysis of Pels. The main role of the calcium ion is the neutralization of the acidic substrate. Four calcium ions located between the enzyme and the substrate are reported in the Ech-PelC–PGA complex structure (Scavetta et al., 1999). The calcium ions and the substrate are located in the T3-PB1 groove of Ech-PelC. However, the calcium ion found in the Pel-15 structure at pH 6.5 (Figs. 1 and 3) is bound to a position (near T3 in the first helical turn) different from that in the Ech-PelC–PGA complex. The major role of the calcium ion of Pel-15 would be in stabilizing the neighbouring T3s in the third and fourth helical turns. Moreover, the longest loop of T3 in the first helical turn is also stabilized indirectly by the calcium ion via a water-mediated interaction with the main-chain carbonyl O atom of Gly34 on the same T3 (Fig. 3). This calcium ion could not be removed by adding 10 mM EDTA to the crystallization buffer. Therefore, this calcium ion is structurally essential for Pel-15, which is a unique feature of Pel-15.

One of the catalytically essential calcium ions found in the Ech-PelC–PGA complex was found as a second calcium ion in Pel-15 when the Pel-15 crystal was soaked in glycine buffer pH 9.5 with 10 mM CaCl₂. The calcium ion is bound in the T3-PB1 groove. This calcium-binding site comprises three residues: Asp63, Glu83 and Asp84 (Fig. 5a). If two of them, Asp63 and Glu83, are individually replaced by other amino acids, Pel-15 loses its pectate-lyase activity almost completely. A similar cluster of acidic residues is found in the Ech-PelC structure. In

the other hand, crystals grown with 10 mM EDTA grew in form II. Although the crystals were grown with EDTA, the calcium ion near Asp80 remained. The differences between these two conditions are the concentrations of the calcium ion and the chloride ion. Therefore, the reason for the difference between two crystal forms is that the amount of negative and positive ions affects the hydrophobic regions of the N- and C-terminal helical coils, diminishing the hydrophobic interaction. This results in the growth of the form I crystal.

3.3. Details of Pel-15 in comparison with Ech-PelC

3.3.1. Side-chain features of the β-helix. An unique feature of Pel-15 is the disulfide bond inside the β-helix. The disulfide bond keeps the β-helix structure of Pel-15 rigid. This type of disulfide bond is not found in Ech-PelC. Although Ech-PelC

this cluster, the side chains of Asp129, Asp131 and Glu166 (in Ech-PelC nomenclature) make a calcium-binding cluster (Fig. 5b). Indeed, a calcium ion is bound to the cluster in the Ech-PelC–PGA complex structure (Scavetta *et al.*, 1999). Therefore, this calcium ion is essential for catalysis of Pel-15 and the T3-PB1 groove may bind the substrate with a mediating calcium ion.

The reason for the detection of the second calcium ion at pH 9.5 only is that the pK_a of Asp63 is raised by the interaction between an N atom of the imidazole group of His66 and an O atom of the carboxyl group of Asp63 (Fig. 5a).

3.3.3. Active site. Fig. 5 shows several residues that Pel-15 and Ech-PelC have in common in the T3-PB1 groove. The acidic residue cluster was discussed in the previous section. This cluster binds the calcium ion, which probably mediates the interaction between the substrate and the enzyme. For the β-elimination reaction, a basic residue is thought to play the key role of abstraction of the C-5 proton from the substrate (Gerlt *et al.*, 1991; Gerlt & Gassman, 1992, 1993). In Ech-PelC, the arginine residue (Arg218) is the key residue in the lyase activity. In addition, the neighbouring lysine (Lys190) residue would be required to stabilize the reaction intermediate (Fig. 5b; Scavetta *et al.*, 1999).

In Pel-15, the basic residues related to the catalysis were examined by site-directed mutagenesis. From the results, three residues, Lys107, Lys129 and Arg132, were found to be candidates for the catalytic residues (Hatada *et al.*, 2000). The comparison of the geometries of these three residues with those of Ech-PelC gives an insight about the roles of those residues (Figs. 5a and 5b). Lys107 is located near the acidic residues cluster comprised of Asp63, Glu83 and Asp84. The geometry near Lys107 is similar to that of Lys190 of Ech-PelC. Therefore, Lys107 of Pel-15 would be required to stabilize the reaction intermediate. There is no residue in Ech-PelC corresponding to Lys129 of Pel-15. This residue may be required for interaction with the substrate. Consequently, Arg132 is attributed to be the key residue which abstracts the C5 proton from the substrate. However, the orientation of the guanidine group of the Arg132 side chain of Pel-15 is different to that of the corresponding residue of Ech-PelC (Figs. 5a and 5b). The guanido group of Arg132 makes a salt bridge with the carboxyl group of Asp161. Moreover, the arginine conformation was not changed even when Pel-15 was soaked in a pH 9.5 solution (where Pel-15 remains active). The basicity of the guanido group of Arg132 may be increased by the interaction with the carboxyl group of Asp161 and the N atom of the guanido group may abstract the proton from the substrate efficiently. Therefore, the conformation of the Arg132 side chain of Pel-15 may not change when Pel-15 interacts with the substrate through breakage of the salt bridge. Consequently, the conformation of the substrate in Pel-15 may be different from that in Ech-PelC.

3.3.4. High alkalinity and low molecular weight. Alkali-resistant bacteria such as *Bacillus* sp. produce many alkaline enzymes. Such alkaline enzymes adapt themselves to alkaline environments by raising their isoelectric points through increasing the number of arginine residues (Shirai *et al.*, 1997).

Pel-15 also increases the ratio of arginine residues to total residues to twice that of Ech-PelC (Yoder, Keen *et al.*, 1993; Yoder, Lietzke *et al.*, 1993).

The adaptation to alkaline environments may explain the low molecular weight of Pel-15. In Pel-15, the long loop protruding from T3 of the first helical turn consists of only 18 residues. Moreover, the N- and C-terminal extensions which are present in Ech-PelC are not found in Pel-15. One reason why Pel-15 acts on PGA at higher pHs may be that Pel-15 utilizes the highly alkaline environment for enzymatic activity. Generally, pectate is slowly chemically degraded at pH 12. Therefore, pectate is likely to be degraded at pH 10.5 without enzymes.

3.4. Absence of N- and C-terminal extensions

An interesting feature of Pel-15 is the absence of the N- and C-terminal extensions which protrude from the β-helix. In general, these extensions are structurally conserved among Pels in polysaccharide lyase family 1. Furthermore, the N-terminal extension contains detectable sequence identities, as seen in almost all β-helix proteins reported thus far (Jenkins *et al.*, 1998). The Pel-15 structure suggests that the lack of such extensions does not affect the polysaccharide binding and enzymatic activity. However, the lack of the N-terminal extension, especially α-helix, is very rare among the L- or V-shaped right-handed β-helix enzymes/proteins. The only N-terminal extension-lacking enzymes/proteins reported thus far are Pel-15 and pertactin (Emsley *et al.*, 1996). In right-handed β-helix enzymes/proteins with the N-terminal α-helix, the hydrophobic side chains of the α-helix interact with the hydrophobic core in the N-terminal part of the β-helix. The folding of right-handed β-helix structures may be initiated with the help of the α-helix. That is, the hydrophobic side chains of the α-helix seem to assist in gathering hydrophobic residues in the first turn of the β-helix. At the same time, the unusual α_L-conformational β-turn may be produced on T2. What initiates formation of the β-helix structure in the N-terminal α-helix-lacking proteins? One suggestion is that a part of the signal peptide region is manipulated. If this region is folded into an α-helix-like motif before secretion, the β-helix structure may be assisted in folding. The N-terminus of the mature Pel-15 protein is at T2. In the other β-helix structures, the N-terminal α-helix starts around T3 and ends around T1. Therefore, in Pel-15 the α-helix exists at least ten residues upstream of the N-terminal end of the mature protein sequence. In the open reading frame −27M to −10Y in Pel-15, there are three regions that are likely to fold into an α-helix, found as L*xxx*L in other β-helix proteins. The signal peptide of Pel-15 is rather long (27 residues). Therefore, it is possible that a part of the signal peptide may assist in folding of the β-helix in Pel-15.

References

Akita, M., Suzuki, A., Kobayashi, T., Ito, S. & Yamane, T. (2000). *Acta Cryst.* D**56**, 749–750.

Brünger, A. T. (1992). *X-PLOR. A System for Crystallography and NMR, Version* 3.1. New Haven, CT, USA: Yale University Press.

Coutinho, P. M. & Henrissat, B. (2000). *Recent Advances in Carbohydrate Bioengineering*, edited by H. J. Gilbert, G. J. Davies, B. Henrissat & B. Svensson, pp. 3–12. Cambridge: Royal Society of Chemistry.

Cowtan, K. (1994). *Jnt CCP4/ESF–EACBM Newsl. Protein Crystallogr.* **31**, 34–38.

Emsley, P., Charles, I. G., Fairweather, N. F. & Isaacs, N. W. (1996). *Nature (London)*, **381**, 90–92.

Fujimoto, Z., Takase, K., Doui, N., Momma, M., Matsumoto, T. & Mizuno, H. (1998). *J. Mol. Biol.* **277**, 393–407.

Gerlt, J. A. & Gassman, P. G. (1992). *J. Am. Chem. Soc.* **114**, 5928–5934.

Gerlt, J. A. & Gassman, P. G. (1993). *J. Am. Chem. Soc.* **115**, 11552–11568.

Gerlt, J. A., Kozarich, J. W., Kenyon, G. L. & Gassman, P. G. (1991). *J. Am. Chem. Soc.* **113**, 9667–9669.

González-Candelas, L. & Kolattukudy, P. E. (1992). *J. Bacteriol.* **174**, 6343–6349.

Guo, W., González-Candelas, L. & Kolattukudy, P. E. (1995*a*). *J. Bacteriol.* **177**, 7070–7077.

Guo, W., González-Candelas, L. & Kolattukudy, P. E. (1995*b*). *Arch. Biochem. Biophys.* **323**, 352–360.

Guo, W., González-Candelas, L. & Kolattukudy, P. E. (1996). *Arch. Biochem. Biophys.* **332**, 305–312.

Hatada, Y., Saito, K., Koike, K., Ozawa, T., Kobayashi, T. & Ito, S. (2000). *Eur. J. Biochem.* **267**, 2268–2275.

Heffron, S., Moe, G. R., Sieber, V., Mengaud, J., Cossart, P., Vitali, J. & Jurnak, F. (1998). *J. Struct. Biol.* **122**, 223–235.

Heikinheimo, R., Flego, D., Pirhonen, M., Karlsson, M. B., Eriksson, A., Mae, A., Koiv, V. & Palva, E. T. (1995). *Mol. Plant-Microbe Interact.* **8**, 207–217.

Henrissat, B., Heffron, S. E., Yoder, M. D., Lietzke, S. E. & Jurnak, F. (1995). *Plant Physiol.* **107**, 963–976.

Huang, W., Matte, A., Li, Y., Kim, Y. S., Linhardt, R. J., Su, H. & Cygler, M. (1999). *J. Mol. Biol.* **294**, 1257–1269.

Jenkins, J., Mayans, O. & Pickersgill, R. (1998). *J. Struct. Biol.* **122**, 236–246.

Knight, S. D. (2000). *Acta Cryst.* D**56**, 42–47.

Kobayashi, T., Koike, K., Yoshimatsu, T., Norihiro, H., Suzumatsu, A., Ozawa, T., Hatada, Y. & Ito, S. (1999). *Biosci. Biotechnol. Biochem.* **63**, 65–72.

Kraulis, P. J. (1991). *J. Appl. Cryst.* **24**, 946–950.

Laskowski, R. A., MacArthur, M. W., Moss, D. S. & Thornton, J. M. (1993). *J. Appl. Cryst.* **26**, 283–291.

Lietzke, S. E., Scavetta, R. D., Yoder, M. D. & Jurnak, F. (1996). *Plant Physiol.* **111**, 73–92.

Merritt, E. A. & Bacon, D. J. (1997). *Methods Enzymol.* **277**, 505–524.

Navaza, J. (1994). *Acta Cryst.* A**50**, 157–163.

Otwinowski, Z. (1991). *Proceedings of the CCP4 Study Weekend. Isomorphous Replacement and Anomalous Scattering*, edited by W. Wolf & A. G. W. Leslie, pp. 80–86. Warrington: Daresbury Laboratory.

Otwinowski, Z. (1993). *Proceedings of the CCP4 Study Weekend. Data Collection and Processing*, edited by L. Sawyer, N. Isaacs & S. Bailey, pp. 56–62. Warrington: Daresbury Laboratory.

Peterson, T. N., Kauppinen, S. & Larsen, S. (1997). *Structure*, **5**, 533–544.

Pickersgill, R., Jenkins, J., Harris, G., Nasser, W. & Robert-Baudouy, J. (1994). *Nature Struct. Biol.* **1**, 717–723.

Pickersgill, R., Smith, D., Worboys, K. & Jenkins, J. (1998). *J. Biol. Chem.* **273**, 24660–24664.

Read, R. J. (1990). *Acta Cryst.* A**46**, 900–912.

Santen, Y. V., Benen, J. A. E., Schröter, K.-H., Kalk, K. H., Armand, S., Visser, J. & Dijkstra, B. W. (1999). *J. Biol. Chem.* **274**, 30474–30480.

Scavetta, R. D., Herron, S. R., Hotchkiss, A. T., Kita, N., Keen, N. T., Benen, J. A. E., Kester, H. C. M., Visser, J. & Jurnak, F. (1999). *Plant Cell*, **11**, 1081–1092.

Shevchik, V. E., Robert-Baudouy, J. & Hugouvieux-Cotte-Pattat, N. (1997). *J. Bacteriol.* **179**, 7321–7330.

Shirai, T., Suzuki, A., Yamane, T., Ashida, T., Kobayashi, T., Hitomi, J. & Ito, S. (1997). *Protein Eng.* **10**, 627–634.

Soliano, M., Blanco, A., Diaz, P. & Pastor, F. I. (2000). *J. Microbiol.* **146**, 89–95.

Steinbacher, S., Seckler, R., Miller, S., Steipe, B., Huber, R. & Reinemer, P. (1994). *Science*, **265**, 383–386.

Yoder, M. D., Keen, N. T. & Jurnak, F. (1993). *Science*, **260**, 1503–1507.

Yoder, M. D., Lietzke, S. E. & Jurnak, F. (1993). *Structure*, **1**, 241–251.